Comprehensive preparation and catalytic activities of Co/TEMPO-cellulose nanocomposites: A promising green catalyst

Nouaamane El Idrissi, Larbi Belachemi, Nicolas Merle, Philippe Zinck, Hamid Kaddami

Comprehensive preparation and catalytic activities of Co/TEMPO-Cellulose nanocomposites: A promising green catalyst

Nouaamane EL Idrissi [1,2], Larbi Belachemi[1], Nicolas Merle[2], Philippe Zinck[2], Hamid Kaddami[1,*]

1- IMED-Lab, Team of Organometallic and Macromolecular Chemistry-Composite Materials, Department of Chemical Sciences, Faculty of Science and Technology, Cadi Ayyad University Marrakech, Morocco.

2- Unité de Catalyse et Chimie du Solide, UMR 8181, Univ. Lille, CNRS, Centrale Lille, Univ. Artois, F-59650, Villeneuve d'Ascq, France

Abstract:

The present study aims to develop a green, cost effective and facile method for the production of cobalt/ 'TEMPO oxidized cellulose' (TEMPO-Cell) heterogeneous catalyst for organic chemical reactions. Indeed, 'TEMPO-Cell' was employed as solid support and stabilizing agent for the highly active cobalt metal particles via *in situ* green and facile preparation method. The process of preparation implied the reduction of cobalt precursors ($CoSO_4$) in TEMPO-Cell water dispersion in ambient conditions in the presence of $NaBH_4$ as reducing agent. It has been clearly shown that the formation of metallic cobalt particles is due to the presence of "TEMPO-CELL" which screens the Co^{2+} ions and prevents their combination with boron. The structure of the aerogel composite Co/TEMPO-Cell aerogel has been analyzed by scanning electron microscopy, energy dispersive spectroscopy, Fourier transform

infrared spectroscopy, transmission electron microscopy and X-ray photoelectron spectrometry. These characterisations show that metallic cobalt particles have nanometric size and are well dispersed in the ‘’TEMPO-CELL’’ aerogel. The hybrid aerogel composites Co/ TEMPO-Cell showed excellent catalytic activity for model reactions such as the reduction of 4-nitroaniline (4-NA), 4-nitrophenol (4-NP) and 2-nitrophenol (2-NP) in water, in the presence of $NaBH_4$. The reaction kinetic has been followed by UV-visible spectroscopy. It was found that this catalyst is good enough to achieve 100% reduction with high reaction rate (6 min full reaction time) and elevated turnover frequency (150 h^{-1}). The aerogel catalyst was easily isolated from the reaction mixture by simple filtration and reused more than ten times without significant loss of its catalytic activity.

Keywords: aerogel composite; cobalt nanoparticles; ion screening; green chemistry; cellulose; catalysis, recyclability.

Highlights :

- ‘’Cobalt(0)/TEMPO oxidized cellulose’’ heterogeneous catalyst was prepared.
- The characterizations have shown nanometric size and good dispersion of Co^0 particles.
- A screening effect of TEMP-Cell, which prevent Co-B components formation, was highlighted.
- High catalytic performances have been shown for the reduction of nitro to amine groups.

- The catalyst retains catalytic activity even after 11 cycles without significant loss of its catalytic activity.

1. Introduction:

The development of green, economic and highly active catalysts is at the heart of the research in catalysis. Heterogeneous catalysis is one of the most promising technology used in chemical reactions and environmental remediation. [1] [2] Metal and metal oxide nanoparticles (NPs) are emerging to be promising candidates due to their excellent catalytic activities for different organic chemical reactions [3]. However, their applications are limited because of their self-agglomeration in solution which reduces their catalytic performances. In addition, they are difficult to recover from the reaction medium. This is a supplementary challenge that limits their application in heterogeneous catalysis in non-supported structure.[4]–[8]

The effective approach to overcome these problems is the immobilization of metal nanoparticles on different materials. [8] In fact, supported heterogeneous catalysts is one of the major focuses of research in catalysis. The supports can be Metal oxides, Silica, Zeolites, Fibers, Ceramic materials, Pillared clays, and polymers notably [2]–[10]. More recently, many research investigations have been directed towards the exploration of sustainable bio resources to be used as support of metallic particles catalysts. Being the most abundant, renewable, ecofriendly, biocompatible and biodegradable natural polymer, cellulose is widely used as a biomaterial support for catalytic systems due to its properties such as high specific area and strength promising good metallic nanoparticles integration. [11]–[15]

On the other hand, important research attention has been paid towards the utilization of the first row transition metals, especially Ni, Co and Fe, as catalyst in organic synthesis. [2], [16], [17] These metals represent advantageous alternative in organic synthesis compared to their equivalent noble metals of the second and third rows which are less abundant and more expensive. More specifically, the catalytic performances of Cobalt ions (either Co^{2+} or Co^{3+}) as well as the less frequently used Co^{0} , have been widely and extensively studied for, oxidations, C−H amination, Allylation, Alkenylation, etc. reactions. [18]–[26] Apart from the organic synthesis, various cobalt oxides based supported catalysts have been explored and extensively studied in high temperatures process, as active in methane catalysis decomposition (CDM) for the production carbon nanomaterials, for example. This enabled to reduce the CDM temperature to the range of 450–800°C [27], [28]. On the other hand, this family of catalysts has been recently tested for water splitting and oxygen evolution or generation [29]–[33].

Regarding the preparation of cobalt oxides (Co_xO_y), it worthy to emphasis that these different oxides are often synthesized by high temperature processes (T>400°C) involving oxidative/calcination of $Co(OH)_2$, formerly prepared by alkaline treatment of Co^{2+} salts ($CoCl_2$, $CoNO_2$ or $CoSO_4$, etc.). Other investigations have been conducted on the preparation of cobalt oxides by heating CO_3Co in vacuum or in CO_2, or by reduction of Co_2O_3 by NH_3 or of Co_3O_4, by Carbon. *Vice versa*, Co_3O_4 can be obtained by the oxidation of CoO. [27]–[33] On the other hand the preparation of metallic Co^{0} from Co^{2+} ions based salts, such as $CoSO_4$, can be achieved at room temperature by reduction reaction in presence of reducing agent such as hydrazine [34], sodium borohydrid [35], etc.

In this work, we developed a novel, simple and eco-friendly biohybrid aerogels based on cellulose derivative (TEMPO oxidized cellulose) as support and cobalt Metallic (Co^{0}) particles as catalyst. The preparation of this biohybrid catalyst passes through the dispersion

of Co^{2+} ion salt ($CoSO_4$) in the TEMPO-cellulose aerogel and its reduction in mild condition using $NaBH_4$ as reducing agent. To the best of the authors knowledge, few studies are dedicated to the catalytic properties of cobalt supported on cellulose and the use of TEMPO-Cellulose as catalyst support for metal nanoparticles has never been reported as far as we know. In comparison to TEMPO-NFC, which production is energy demanding due to the mechanical defibrillation, the use of TEMPO-cellulose is a simple and novel way to endow cellulose with carboxylic groups that enhance the screen of Co^{2+} cation to permit its reduction to Co^0 in presence of Borate anions. Compared to other nanocelluloses, this TEMPO-cellulose can be efficient to produce stable, efficient Co^0 supported catalyst. The morphology of this composite aerogel is characterized and its catalytic performances for the reduction of nitro-functionalized molecules to amino-functionalized ones were tested.

2. Material and Methods

Chemicals and starting materials:

The rachis of date palm tree (*Phoenix dactylifera L.*) was used in this work as the original source of cellulose. Cellulose was extracted from the rachis following the procedure well described in our previous work. [36]

TEMPO (1-oxo-2,2,6,6-tétraméthylpipyridine1-oxyle) , sodium bromide, sodium hypochlorite solution (15%), HCl, NaOH, Cobalt (II) sulphate heptahydrate [$CoSO_4.7H_2O$], Sodium borohydride $NaBH_4$, 4-nitroaniline (4-NA), 4-nitrophenol (4-NP) and 2-nitrophenol (2-NP) were purchased from Sigma–Aldrich and used without further purification.

Preparation of the TEMPO-Cell

The rachis of date palm tree was used in this work as the original source of cellulose. TEMPO mediated oxidation was performed following the procedure well described in our previous work [37], [38]. About 2 g, *i.e.* 2.136 mmol of equivalent anhydroglucose unit (AGU) of cellulose, were suspended in water (200 mL) and sonicated with a Branson Sonifier for 5 min. TEMPO (32 mg, 0.065 mmol) and NaBr (0.636 g, 1.9 mmol) were added to the suspension. A certain amount of the NaOCl solution, corresponding to 40.5 mL was added drop wise to the cellulose suspension. The pH was adjusted at 10 by addition of a 0.1 M aqueous solution of HCl. The pH of the mixture was maintained to 10 at 4 °C by continuous adding of 0.1 M NaOH while stirring the suspension. After times ranging from 120 min, the oxidation was terminated by adding methanol (5 mL) and the pH was adjusted to 7 by adding 0.1 M HCl. The concentration of carboxylic acid groups has been calculated using conductimetric titration and the carboxylic content found is of 750 µmol/g; in agreement with our previous results [38].

Preparation of TEMPO-Cell based aerogels and catalysts

Porous (Co/ TEMPO-Cell) aerogel composite was prepared by an environmentally friendly method. ($CoSO_4$, $7H_2O$) was added to a dispersion of 1wt% of TEMPO-Cell in water (the amount of ($CoSO_4$, $7H_2O$) was adjusted to obtain an aerogel composite (Co/ TEMPO-Cell) with 4wt% of Cobalt metal :1g of TEMPO-Cellulose, 0.19 g of (CoSO4, 7H2O) was added). Then, sodium tetrahydroboride $NaBH_4$ in distilled water was added. The amount of $NaBH_4$ was calculated to have a stoechiometric ratio of 6M equivalent / Co. The dispersion turns immediately from pink to black colour. After that, the water was eliminated by lyophilisation after freezing the dispersion at -20°C during one night. The neat TEMPO-Cell aerogel was prepared lyophilisation method in the same conditions as for the supported catalyst.

The Co/TEMPO-Cell aerogel composite catalyst was prepared by the following reaction sequences which is described in the following S1 (Supporting data S1). The first step relates to the oxidation by NaOCl + NaBr + TEMPO mixture followed by treatment with cobalt sulphate $CoSO_4$ in aqueous solution and reduction with $NaBH_4$ (Supporting data S1).

Characterization techniques

Infrared spectra were recorded on a FT-IR Perkin-Elmer 1000 spectrometer collecting 32 scans from 400 to 4000 cm^{-1}. Transmission FTIR was performed on KBr based pellets prepared from grinded sample and KBr power. A separate background spectrum was collected and automatically subtracted from the raw spectrum for each specimen.

A Philips X'per wide angle X-ray diffractometer operated at 40 kv and 30 mA with a Ni-filtered CuKα radiation was used to determine the crystallinity index of the specimens. X-ray diffractograms were recorded at 0.02° s^{-1} over a 2θ diffraction angle scan in the range 5–90°. XRD was performed, especially, to check the metallic structure of Co in the aerogel.
The model TESCAN – VEGA3, with accelerating voltage of 12.5 kV was used. A piece of aerogel was deposited on a SEM support and coated with a thin layer of carbon. EDX measurement was performed using AMETEK, EDAX- OCTANE PLUS.
The UV–vis spectra was used to study the kinetics of the reaction of reduction 4-Nitroaniline catalysed by TEMPO-Cell/Co catalyst. The spectra were taken at room temperature from 200 to 520 nm using a Shimadzu UV–vis spectrometer (UV-2450).

TEM

Transmission electron microscope FEI-Tecnai G2 operated at an accelerating voltage

of 200 kV was used for the morphological observation.

TEM sample was prepared by depositing two to three drops of (1 mg/1 mL) Co/TEMPO-Cellulose suspensions on carbon-coated electron microscope grids and dried at ambient temperature.

XPS

XPS analyses were performed by a Kratos Axis Ultra DLD spectrometer with monochromatized Al Kalpha X-rays operating at 180 W (12 mA and 15 kV).

Catalytic Reduction of nitro-functionalized molecules

'' An aqueous solution of 0.5 g/L NFM (nitro-functionalized molecule: 4-nitroaniline, 4-Nitrophenol or 2-Nitrophenol) is prepared, which correspond to 3,5 mM solution of NFM. For each reaction test, a 10 mL of this solution of NFM in water was used, in which an amount corresponding to 10 equivalents of $NaBH_4$ vas added. An amount of aerogel catalyst Co/TEMPO-Cell, respecting the ration N(Co)/N(NFM)=0.05 was then added. The mixture is mildly stirred at room temperature. In these condition Molar ratio of NaBH4 / NFM / Catalyst is 1000 / 100 / 5 ''.

Kinetic studies by UV-Visible spectrometry

The kinetic monitoring of the reaction by UV-Visible spectrometry requires the establishment of a calibration curve to convert the absorbance into concentration of the studied solution. Thus, we prepared solutions of NFM with different concentrations and we scanned the absorbance as a function of the wavelength (supplementary data S1-left). Monitoring the evolution of the intensity of the absorption band at 400 nm at the absorption maximum as a function of concentration allows us to obtain the calibration curve presented in S1-right. A

straight line obtained by the origin and which therefore verifies the law of Beer Lambert. This calibration curve is used to study the kinetics of NFM reduction reaction.

3. Results and discussion

A. Aerogels Characterization

The morphology of Co/TEMPO-Cell was characterized by mean of scanning electron microscopy (SEM-EDX), FTIR spectroscopy, X-ray diffraction (XRD) and XPS.

Figure 1 shows the SEM pictures of pure TEMPO-Cell aerogel taken as reference and those of the Co/TEMPO-Cell aerogel composite with different magnifications. The optical photos of the aerogels are also presented to show their macroscopic aspect (figures 1-A and 1-B). The SEM micrograph of cross section of the aerogel made of pure TEMPO-Cell aerogel shows the presence of micrometric fibers of 6-8 µm of diameter surrounded with films (figures 1-C and 1-E). These films are certainly formed of oxidized cellulose fibrils which were disintegrated from the bleached cellulose fibers during the TEMPO mediated oxidation process. In fact, it's well known that TEMPO mediated oxidation of cellulose fibers facilitated the dissociation of cellulose nanofibrils owing to the repulsive interactions developed between the carboxylate groups created [38], [39]. These fibrils are then assembled and organized as a film during the freeze-drying process. In this structure the film ensure good connection and cohesion of the aerogel network which enables obtaining monolith aerogel [40]. Similar structure can be observed in SEM image of Co/TEMPO-Cell presented in Figures 1-H, 1-J and 1-L with the presence of small particles (diameter lower than 200 nm), homogeneously dispersed in the films (Figure 1-J). These particles are certainly composed of Co metal since they are absent in the pure TEMPO-Cell aerogel. The

observation of the Co/TEMPO-Cell aerogel at higher magnifications (figures 1-J and 1-L) enabled to better distinguish these particles and to show that they are homogeneously dispersed in the films of cellulose. It is worthy noticing that bigger particles (diameter up to 2 µm) are also observed, and they are certainly formed by the aggregation of the nanometric ones.

EDX analyses (Figure 1- K and L) confirm that these particles are composed of cobalt. At that level the type of interaction between the TEMPO-cell and the metal particle is of high importance. SEM analyses cannot give information about this inquiry. However, in our approach the cobalt particles are fixed and stabilized by the hydrogen bonds to the TEMPO-Cell surface. It can easily be understood that the carboxylate groups at the TEMPO-Cell surface play an emulsifying effect to control the size and insure good dispersion of cobalt particles in the aerogel. The 2D-EDX elemental mapping enabled to show that the cobalt is homogeneously distributed in the composite aerogel (supporting data S2).

A : Optic photo of pure TEMPO-Cell aerogel

B : Optic photo of Co/ TEMPO-Cell aerogel

C: Pure TEMPO-Cell aerogel : Magnification of 500

D: Co/ TEMPO-Cell aerogel : Magnification of 500

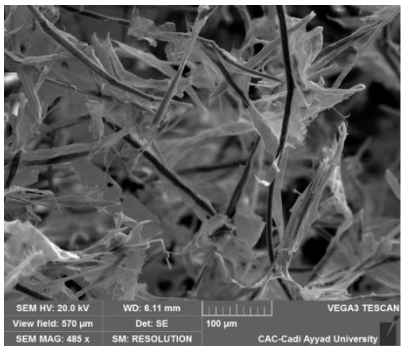

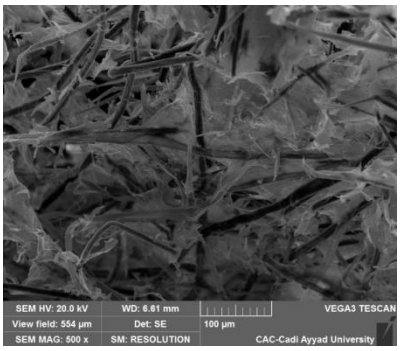

E: Pure TEMPO-Cell aerogel : Magnification of 2000

F: Co/ TEMPO-Cell aerogel : Magnification of 2000

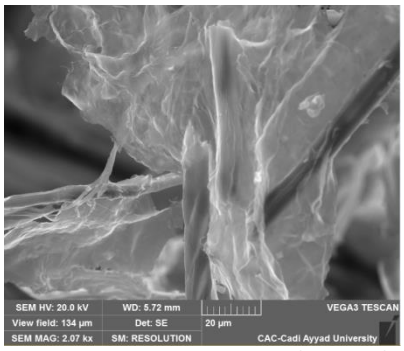

G: *Pure TEMPO-Cell aerogel : Magnification of 10000*

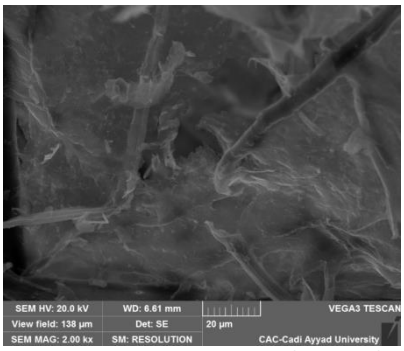

H: *Co/ TEMPO-Cell aerogel : Magnification of 10000*

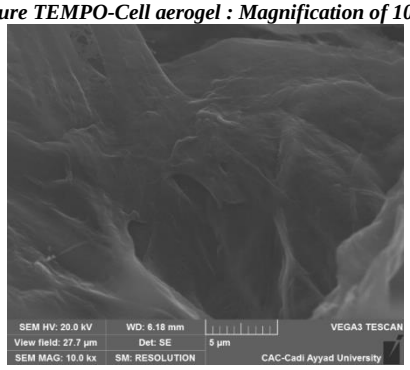

I: *Pure TEMPO-Cell aerogel : Magnification of 20000*

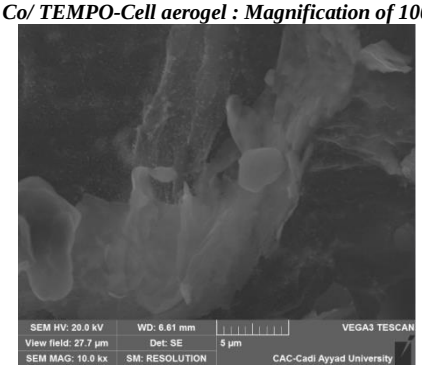

J: *Co/ TEMPO-Cell aerogel : Magnification of 20000*

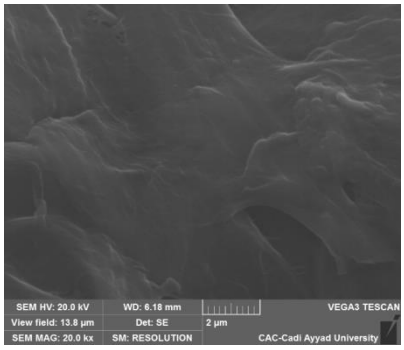

K: EDX of *Pure TEMPO-Cell aerogel*

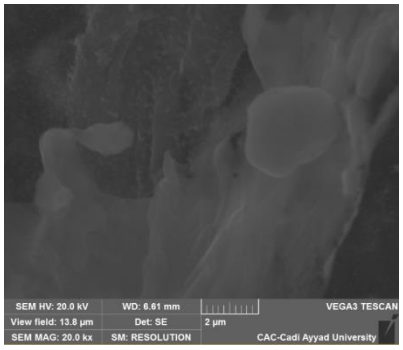

L: EDX of *Co/ TEMPO-Cell aerogel*

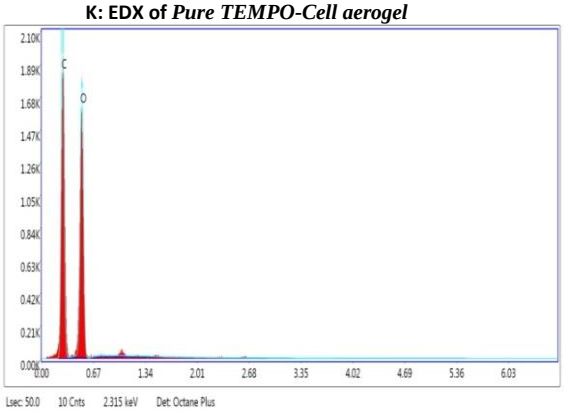

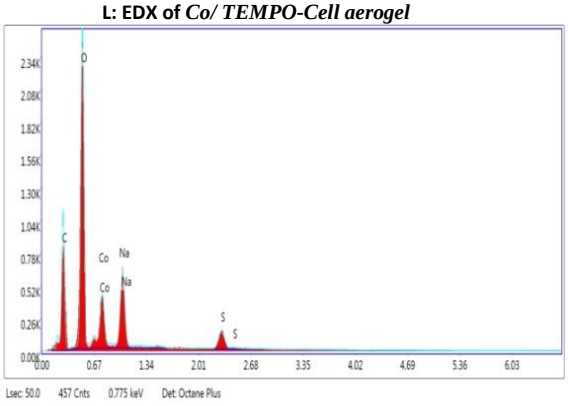

Figure 1: Optical, MEB and EDX characterizations of the TEMPO-Cell and Co/ TEMPO-Cell composite aerogels

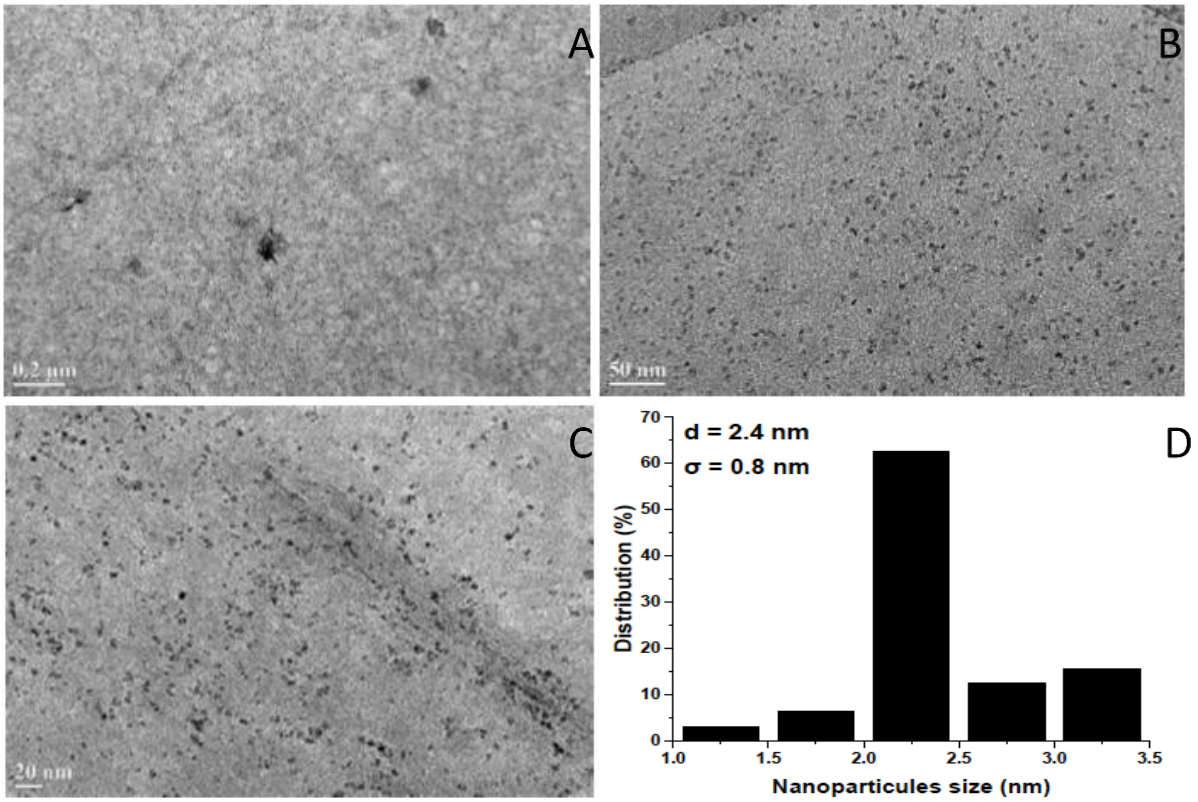

Figure 2: TEM images of Co/ TEMPO-Cell composite aerogels and Cobalt nanoparticles diameter distribution

To have a clear idea about the formation of cobalt nanoparticles observed in the aerogels by SEM analyses, the dispersion of TEMPO oxidized cellulose supported cobalt nanoparticles was diluted in water, transferred to a carbon grid, dried in a vacuum overnight to dry and finally observed by TEM.

As shown in the Figure 2, the cobalt nanoparticles are almost less than 4 nm in diameter and are well dispersed on the whole TEMPO-cell film. Their mean diameter (d) and standard deviation (σ) were estimated to be 2.4 and 0.8 nm, respectively. These particles are very small compared to those obtained in literature (see comparison in Table 1). This shows that, in comparison to the conventional NCC and NFC nanocelluloses, the TEMPO-cell has a

pronounced emulsifying and stabilising effects, which enables the obtaining of very fine and well-dispersed metallic nanoparticles.

Table 1: Comparison of the metal nanoparticles size with other reported systems

Metal	Nanoparticles size (nm)	Precursor	synthesis method	Support	Application	Reference
Au	15.6	$HAuCl_4$	reduction by NFC	NFC	Catalyst	Alle and al. [41]
Au	12-19	$HAuCl_4$	reduction by NCC	NCC	glucose detection	Alle and al. [42]
Au Ag	18-25 6-35	$HAuCl_4$, $AgNO_3$	reduction by ascorbic acid	NCC	Catalytic reduction of nitrophenol	Eisa and al. [9]
Au Pd	15-30 20	$HAuCl_4$ $PdCl_3$	reduction by dialdehyde NFC	NFC	suzuki coupling reaction	Zhang and al. [43]
Ag	10-20	$AgNO_3$	Sodium citrate	CMC/NCC	Antibacterial properties	Yunqing and al. [44]
Ag	10-100	$AgNO_3$	reduction by $NaBH_4$	NCC	sensors, catalysts, and conductive material	Dafne and al. [45]
Pd	6	$PdCl_2$	$NaBH_4$	NFC	Catalyst	Meng and a., [46]
Cu	14.65	$CuSO_4$	reduction by hydrazine	NCC	Catalytic oxidation of sulfides and alcohols	Dutta et al. [47]
Cu	7	$CuSO_4$	reduction by $NaBH_4$	NCC	C-N coupling reactions	Goswami and al. [48]
Co	**2.4**	**$CoSO_4$**	**reduction by $NaBH_4$**	**TEMPO-Cellulose**	**Catalytic reduction reactions**	**This work**

A

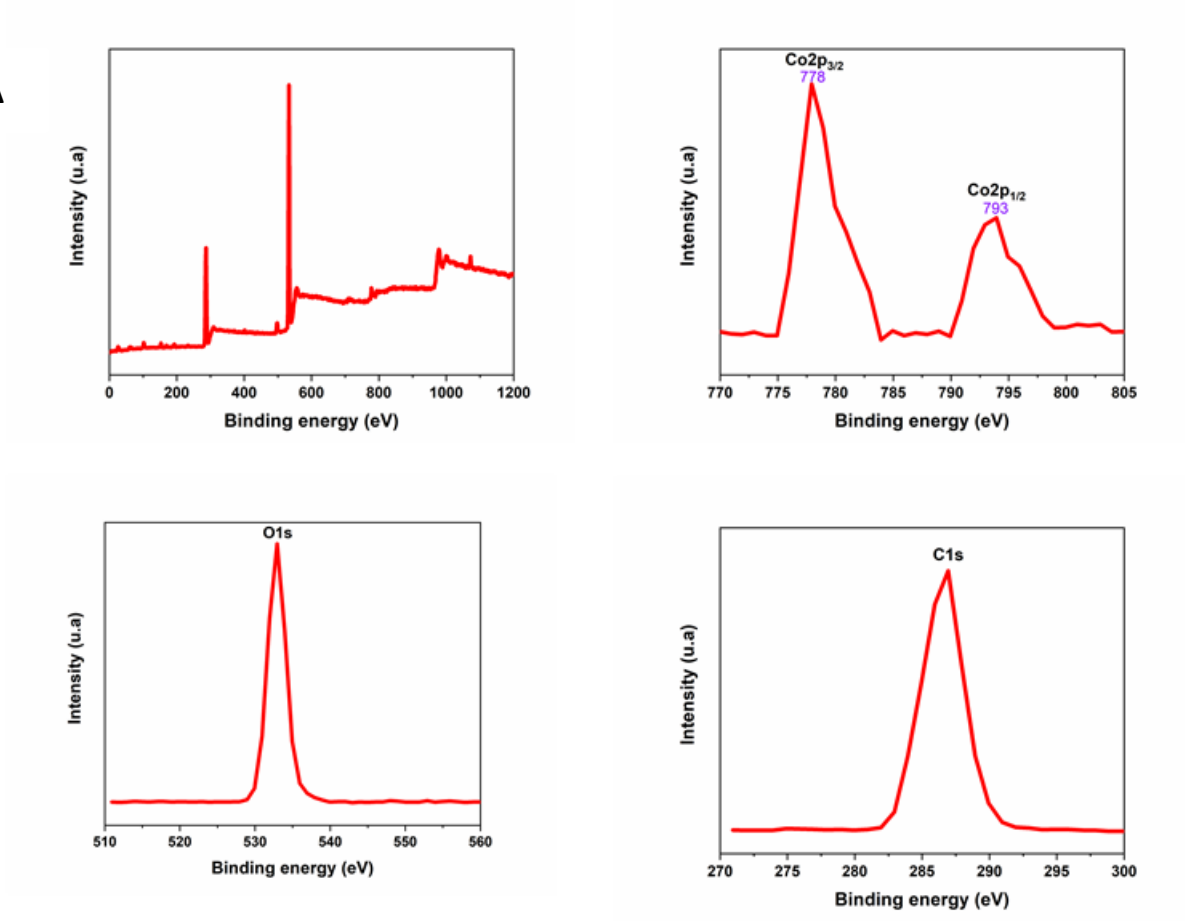
Intensity (u.a)
0
200
400
600
800
1000
1200
Binding energy (eV)
Co2p3/2
778
Co2p1/2
793
Intensity (u.a)
770
775
780
785
790
795
800
805
Binding energy (eV)
O1s
Intensity (u.a)
510
520
530
540
550
560
Binding energy (eV)
C1s
Intensity (u.a)
270
275
280
285
290
295
300
Binding energy (eV)

242

243

244

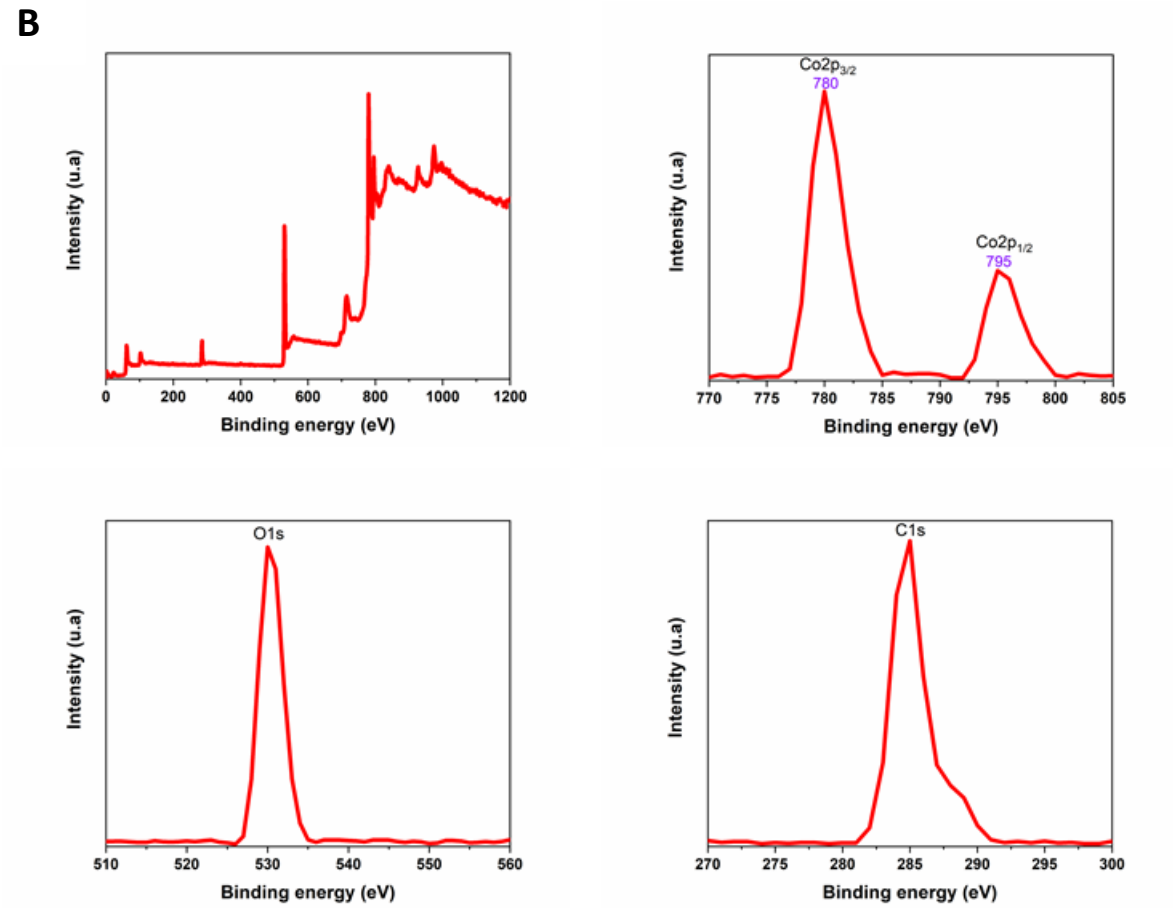

Figure 3: XPS of A: Co/TEMPO-Cell B: synthesized CoB

To ensure of the metallic structure of the observed nanoparticles, XPS analysis on the composite aerogel Co/TEMPO-Cell was performed. Figure 3-A shows the XPS spectrum obtained. The Co2p1/2 and Co2p3/2 peaks of Cellulose-TEMPO supported Cobalt nanoparticles were analyzed. Various cobalt oxidation peaks, that have been reported in the literature, [49] are 778.3 and 793.3 eV for Co^0, 780.4 and 795.8 eV for Co^{2+} and 778.5 and 794.2 eV for Co^{3+}. Accordingly, the metal nanoparticles of the studied Co/TEMPO-Cell show a Co2p3/2 base level peak at a binding energy of 778.3 eV, and Co2p1/2 at 793.3 eV, confirming the presence of the typical valence state of metallic Co^0 (Figure 3-A).

Figure 3-B shows different XPS peaks compared to the pure metal. The amorphous CoB shows a peak for Co2p3/2 at 780.2 eV, which indicates that some electrons are transferred from Co to B, based on their electronegativity. [50]

The FTIR spectra of the Co/TEMPO-Cell composite aerogel and the pure TEMPO-Cell aerogel are presented in figure 4 and show characteristic vibration bands of the OH stretching at 4000–2995 cm^{-1}, the OH bending of adsorbed water at 1635 or 1638 cm^{-1}, the CH stretching at 2900 cm^{-1}, the HCH and OCH bending vibrations at 1430 cm^{-1}, the CH deformation vibration at 1375 cm^{-1}, the stretching vibration of C=O from the free COOH band near 1737 cm^{-1}, the C–OH bending mode at 668 cm^{-1}. Comparing the two spectra, it observed that the stretching vibration of C=O from the free COOH band at 1737 cm^{-1} disappears. Furthermore, the intensity of the band of C–OH bending mode at 668 cm^{-1} strongly increases. These observations confirm that the COOH and OH groups of cellulose are in interactions with cobalt nanoparticles, [51], [52].

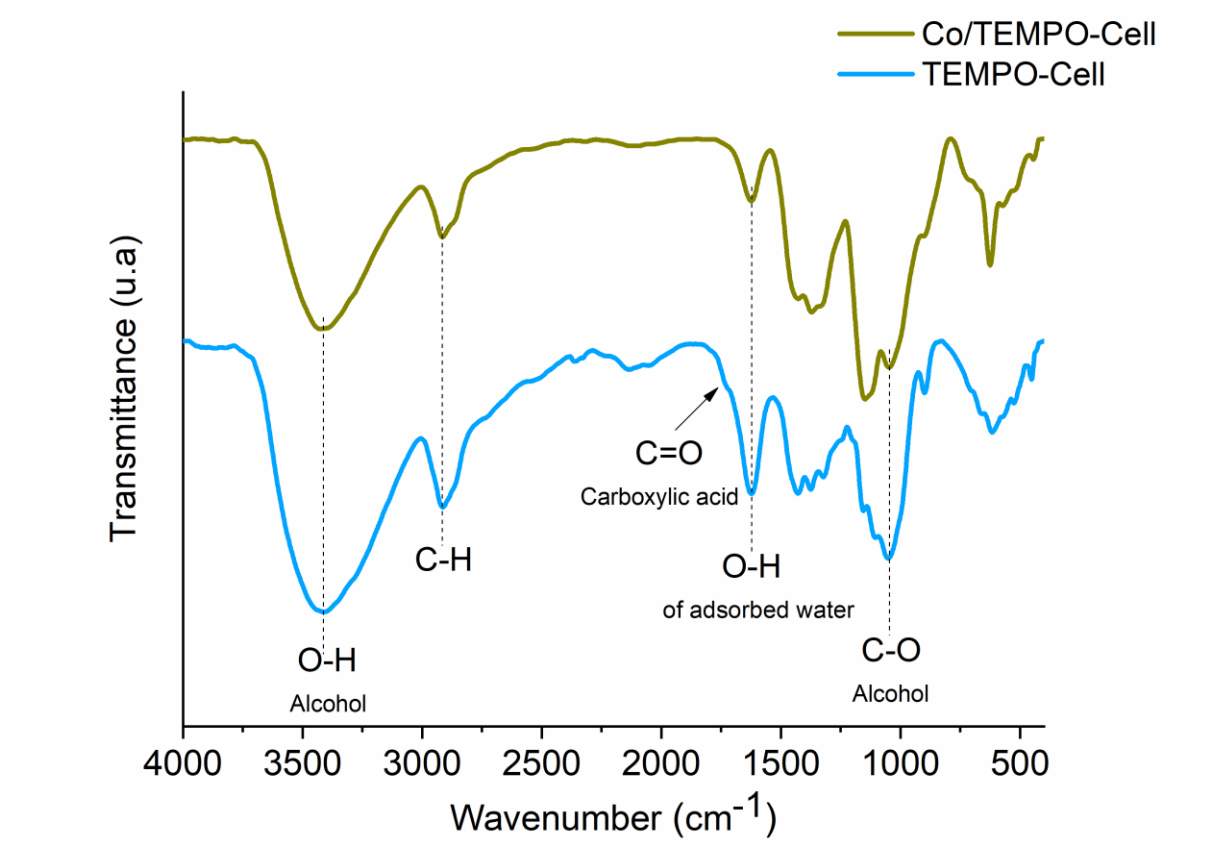

Figure 4: FTIR spectra of TEMPO-Cell and Co/ TEMPO-Cell composite aerogel.

Several reports of the literature have shown that the reduction of cobalt(II) in homogeneous media with borohydride is very complicated. [53]

To emphasis the effect of TEMPO-Cell on Co^0 metallic nanoparticle during the reduction with borohydride, a reduction of Co^{2+} ions ($CoSO_4$, $7H_2O$) in water (without TEMPO-Cell) using $NaBH_4$ in the same conditions as for the preparation of borohydride Co/TEMPO-Cell has been performed (use of sodium $NaBH_4$ in distilled water and the amount of $NaBH_4$ was calculated to have a stoichiometric ratio of 6M equivalent/Co). We reported in Figure 5-A (lower spectrum) the XRD spectra of cobalt-based powder obtained. This spectrum shows that the resulting material is amorphous since no diffraction pick could be detected. In contrast, the XRD of Co/TEMPO-Cell composite, presented in Figure 5-B (upper spectrum), shows a crystalline structure of Co^0 in its hexagonal polymorph, as indexed using Cobalt

(JCPDS: 03-056-9722) crystal phase using High Score program. This enables to attribute the high intensity peaks observed at 2Θ= 37.5 and 43.8 to the plans 301 and 220 of hexagonal metal structure of cobalt.

According to Suraj Gupta et al. [54] and Y.D. Wang et al [55] who prepared Cobalt based powder following similar procedure, this cobalt based powder is a Co-B amorphous materials. The XPS analyses of this material show that the cobalt and bore metals exist in both elemental and oxidized state [54]. In this structure, boron acts as the sacrificial agent in order to partially protect Co from oxidation. This clearly indicates the strong interaction between Co and B in CoB and Co2B boride cobalt.

At this stage, it's interesting to compare the reactivity of Co^{2+} toward the reductive action of sodium borohydride in presence and in absence of TEMPO-oxidized cellulose. It's clear that cellulose has an influence in the orientation of the catalytic reduction reaction and the development of Co hexagonal metallic structure instead of Co-B and Co2B amorphous cobalt borides components. It's clear that the strong interaction between B and Co in Co-B component prevent the growth of crystalline structure of metallic Co (Hexagonal or Cubic allomorphs). In presence TEMPO-Cell, the interactions between the hydroxyl, aldehyde and carboxylate groups of TEMPO-Cell and the cobalt (II) and BH_4^- ions causes a high chemoselectivity which directs the reduction reaction towards the formation of cobalt (0) nanoparticles exclusively by screening the Co^{2+} ions and preventing the formation of CoB and Co2B which are usually observed in this type of reduction observed in the absence of TEMPO-oxidized cellulose.

However, it's important to emphasise that TEMPO-Cell itself is not able to reduce the Co^{2+} ions to Co^0 although it contains aldehyde and alcohol groups because of the lower value of the redox potential of the redox couple Co^{2+}/Co^0(-0.28 V) compared to that of redox couples aldehyde/alcohol (-0.2 V) and that of acid/aldehyde (-0.12 V) [56], [57] But, it clearly appears that these organic groups present in TEMPO-Cell have an important role in specifically guiding the reduction of Co^{2+} ions and the formation of Co^0 hexagonal. To this end, these hydroxyl, acid and aldehyde groups which are present at the surface of the TEMPO-oxidized cellulose matrix actively contribute to the selectivity of the catalytic reduction reaction for Co^{2+} to Co^0.

To further understand and confirm the above interpretation, hydrazine was used as reducing agent for the non-supported catalyst. The obtained metal consists of Co^0 with a cubic structure as revealed by XRD analysis presented in Fig. 5-A (upper spectrum). In fact, the XRD spectrum of the powder obtained from the reduction of $Co(SO_4)$ by hydrazine reduction shows many peaks that are related to metallic cobalt particle. All diffraction peaks were indexed using Cobalt (JCPDS: 03-056-9722) crystal phase. These peaks are compared to standard data using the High Score program which allows us to attribute the high intensity peaks observed at 2Θ= 44.57, 51.57, 75.98 and 92.66 to the plans (111), (200), (220) and (311) of cubic metal structure of cobalt. [58]

A

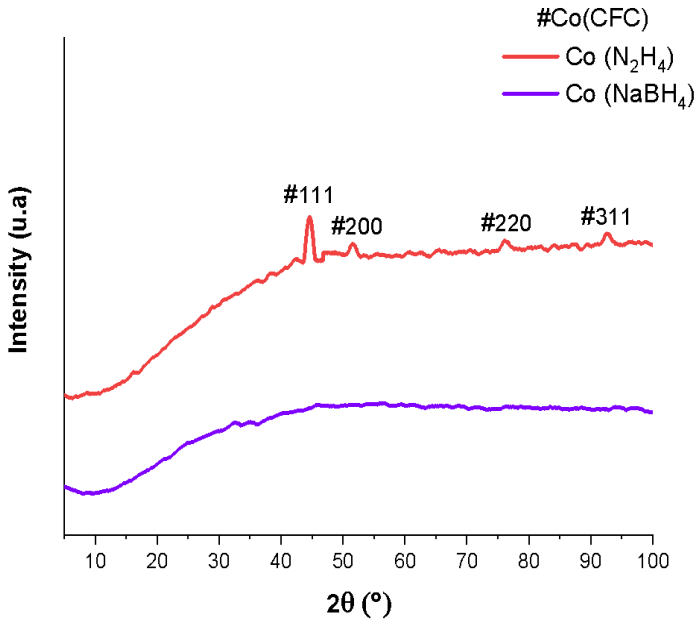
#Co(CFC)
Co (N_2H_4)
Co ($NaBH_4$)
#111
#200
#220
#311
Intensity (u.a)
10 20 30 40 50 60 70 80 90 100
2θ (°)

B

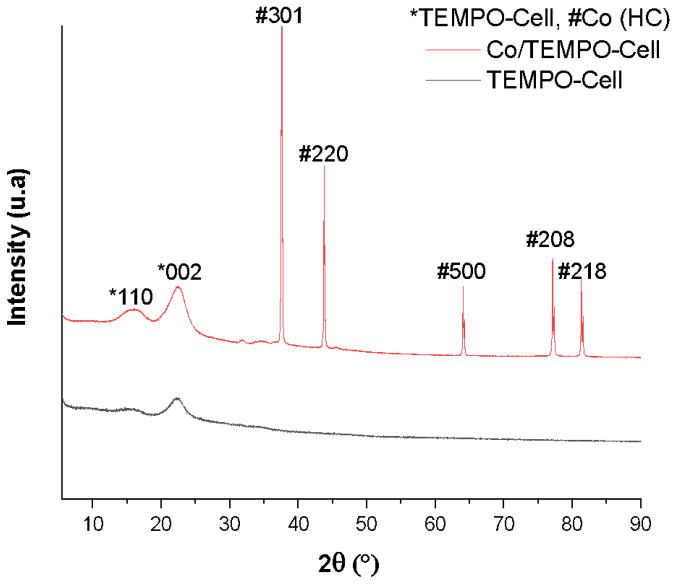
*TEMPO-Cell, #Co (HC)
Co/TEMPO-Cell
TEMPO-Cell
#301
#220
#208
#218
#500
*002
*110
Intensity (u.a)
10 20 30 40 50 60 70 80 90
2θ (°)

Figure 5: XRD analyses; A: XRD of the powders obtained by the reduction of $CoSO_4$ using $NaBH_4$ and Hydrazine; B : XRD spectra of the Co/TEMPO-Cell composite and TEMPO-Cell aerogels

the inducing role of the chemoselectivity of TEMPO-oxidized cellulose for the reduction reaction can be advanced from these results, which prevents the physical rapprochement and the linkage between B and Co entities, promotes the development of Co hexagonal metallic structure as indicated by DRX analyses. In fact, the TEMPO-Cell matrix represents a very important asset for controlling the reduction reaction of cobalt(II) ions and orienting it chemoselectively towards the cobalt(0) nanoparticles which are immobilized on the surface of the matrix, avoiding the formation of CoB which is much less active as a catalyst.

B. Catalytic Activity

After preparation and characterization of the composite aerogel Co/TEMPO-Cell, the catalytic activity and performances were evaluated towards the reduction in aqueous medium of 4-nitroaniline (4-NA), 4-nitrophenol (4-NP) and 2-nitrophenol (2-NP) to para-aminoaniline (4-AA), 2-aminophenol (4-AP) and 2-aminophenol (2-NP), respectively, (Supporting data S3). Para-aminoaniline is an aromatic diamine used in many application including the synthesis of Kevlar [59] and dyes matrices [60], [61], while aminophenols are biologically active and are used in the pharmaceutical industry [62].

The [Co]:[PNA]:[equivalent of $NaBH_4$] molar ratio was fixed at 5:100:1000 and the kinetics were monitored by UV–Vis absorption. The 4-NA/$NaBH_4$ solution displays a strong absorption band at 380 nm, attributed to 4-NA, which was used to follow the kinetics of the reaction.

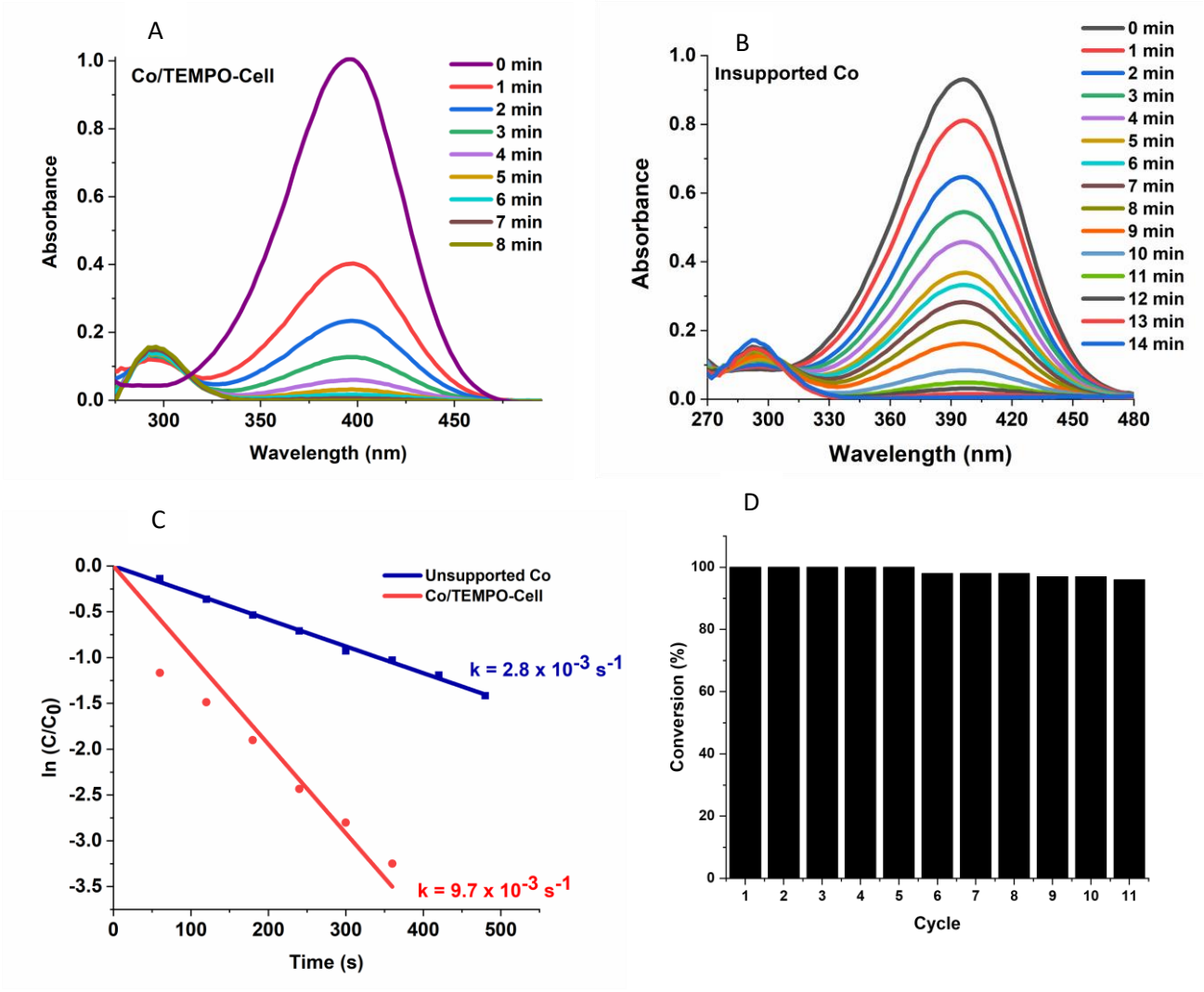
A
Co/TEMPO-Cell
Absorbance
Wavelength (nm)
0 min
1 min
2 min
3 min
4 min
5 min
6 min
7 min
8 min
B
Insupported Co
Absorbance
Wavelength (nm)
0 min
1 min
2 min
3 min
4 min
5 min
6 min
7 min
8 min
9 min
10 min
11 min
12 min
13 min
14 min
C
Unsupported Co
Co/TEMPO-Cell
k = 2.8 x 10-3 s-1
k = 9.7 x 10-3 s-1
ln (C/C0)
Time (s)
D
Conversion (%)
Cycle

Figure 6: A and B : UV-Vis spectra for the reduction of 4-NA with $NaBH_4$ in aqueous solution recorded every 1 min using Co/TEMPO-Cell aerogel composite and unsuported Co catalysts, respectively, C: plots of $\ln[C_t/C_0]$ versus reaction time for the two reduction reaction and D: results of the recyclability tests of the reduction of 4-NA with $NaBH_4$ in presence of Co/TEMPO-Cellulose

The time-dependent UV–vis absorption spectra of the reaction medium during the 4-NA reduction catalyzed by Co/ TEMPO-Cell composite and non-supported catalyst particle are shown in Figures 6-A and 6-B. Regardless the catalyst, one can observe a reduction in the 380 nm absorption with time, confirming the gradual reduction of 4-NA into 4-AA. (8 min) This was accompanied by the apparition and the intensity increase of a new UV absorption band at 302 nm attributed to 4-AA. Surprisingly, even a very low amount of supported catalyst was found to be good enough to achieve 100% reduction of para-nitroaniline with a higher reaction rate However, with the non-supported Co catalyst, the reaction rate is lower and the reduction of 4-nitroaniline is achieved after 14 minutes (Figure 6-B).

The plot of (C_t/C_0) as a function of reaction time, where C_0 and C_t represent the concentrations at t = 0 and t of 4-NA in the reaction medium, are presented in figure 6-C shows a linear relationship for the kinetics with the two catalysts (Co/TEMPO-Cell composite and non-supported catalyst). This can be explained by the fact that the kinetic of this reaction is governed by the reagent contact with the catalytic surface which limits the number of molecules that can react at the same time.

The linear correlation between $\ln(C_t/C_0)$ and time at 295 °K shows that the reduction of 4-NA, 2-NP and 4-NP by Co/TEMPO-Cell /$NaBH_4$ follows the pseudo-first-order reaction kinetics.

The kinetic reaction rate constants (k_{app}) were estimated from the slope of the ln(C_t/C_0) versus time liner curve. Pseudo-first order rate constant could be calculated by Langmuir–Hinshelwood equation [11].

$$Ln(C_t/C_0) = \ln(A_t/A_0) = -k \times t$$

where, k is the rate constant. C_0 and C_t represents the initial concentration of 4-NA, 4-NP and 2-NP and the concentration at time t, respectively. A_0 is the initial absorbance and A_t is the absorbance at any time t.

During the reaction, and notably in the beginning when the concentration of the substrate is much higher than the concentration of the catalyst, the catalyst surface is rapidly occupied by the substrate molecules and remains saturated during the reaction rending the reaction rate to appear constant throughout the reduction period. From these results, the apparent rate constant, k_{app}, was calculated as the slope of the linear plot of (C_t/C_0) versus time. The turnover frequency (TOF, defined as the number of moles of 4-NA reduced per mole of catalyst per hour) could then be evaluated from k_{app}, to compare the catalytic performances of the two catalysts (Table 2). The TOF of Co/ TEMPO-Cell composite aerogel is 200 h^{-1}, while that of non-supported Co catalyst is 80 $h^{-1}$for 4-NA (Table 2).

Similar trends are observed while studying the kinetic of reduction of 2-nitrophenol (2-NP) and 4-nitrophenol (4-NP). The results are presented in supporting data S4 and in Table 2.

Table 2: Comparison of the reducing ability of Co/TEMPO-Cell aerogel composite in reduction of nitro-functionalized molecule (NFM) with other reported systems

*CTAB : hexadecyltrimethyl ammonium bromide

** P(2-acrylamido-2- methyl-1-propansulfonic acid)–Ni nanoparticles hydrogel

Support system	Catalyst	NFM	Molar ratio of $NaBH_4$/NFM/Catalyst	TOF (h^{-1})	Recyclability (number of cycles)	Reference
Graphene hydrogel	Au	4-nitrophenol	460/2,3/1	12	1	Li, Liu, and Liu [65]
Chitosan	Au	4-nitrophenol	20/6/1	50	11	Chang and Chen [66]
CNCs	Au	4-nitrophenol	9819/31,6/1	641	1	Wei Yanaand al. [67]
Poly(methyl methacrylate)	Au	4-nitrophenol	22500/15/1	89	1	Kyoko Kuroda and al. [68]
CNCs	Ag	4-nitrophenol	9/0,3/1	420	3	W. H. Eisa and al. [9]
MCC/CTAB*	Ag	4-nitrophenol	150/15/1	545	1	X. An and al. [69]
2-acrylamido-2-methyl-1-propansulfonic acid	Cu	4-nitrophenol	60000/1500/1.7	74	1	N. Sahiner and al. [70]
P(AMPS)**– hydrogel	Ni	4-nitrophenol	150/7/1	142	5	N. Sahiner and al. [71]
Cell-TEMPO	**Co**	**4-Nitroaniline**	**1000/100/5**	**200**	**11**	**This work**
Unsupported catalyst	**Co**	**4-Nitroaniline**	**1000/100/5**	**86**	**-**	**This work**
Cell-TEMPO	**Co**	**4-nitrophenol**	**1000/100/5**	**154**	**11**	**This work**
Unsupported catalyst	**Co**	**4-nitrophenol**	**1000/100/5**	**86**	**-**	**This work**
Cell-TEMPO	**Co**	**2-Nitrophenol**	**1000/100/5**	171	**11**	**This work**
Unsupported catalyst	**Co**	**2-Nitrophenol**	**1000/100/5**	**86**	**-**	**This work**

We clearly observe that the performances of Co/TEMPO-Cell composite aerogel for the reduction reaction of nitro group are higher in comparison to non-supported catalysts. This can be explained by the fact that the immobilization of particles on a cellulosic support increases surface area and makes cobalt metal nanoparticles more accessible to such nitrobenzene derivatives. The high specific area of cellulose and nanocellulose aerogels and their composites have been widely reported in literature; it has been shown that high values such 100 m^2/g and 200 m^2/g can be reached for these cellulosic aerogels[72-74]. Moreover, in the case of unsupported catalyst, the aggregation and agglomeration of particles

significantly decreases their specific surface area, and limits their reagent accessibility. Consequently, their reactivity is reduced even in the presence of an excess of $NaBH_4$. The comparison of the two unsupported catalyst shows that the crystalline metallic form of cobalt is more effective than unsupported catalyst for this reaction.

Overall, the present Co/TEMPO-Cell catalyst shows greater efficiency for the catalysis of the reduction reaction of nitrobenzene derivatives when compared to previously reported systems (Table 2). We conclude that the TEMPO-oxidized cellulose plays a very important role in controlling the reduction reaction of cobalt(II) ions and orienting it chemo-selectively towards the cobalt nanoparticles which are immobilized on the surface of the matrix. The other possible reasons for the better catalytic activity could be (i) small size of the metallic cobalt nanoparticles, (ii) strong interaction between metallic cobalt nanoparticles and support owing to the presence of many carboxylic, aldehyde and hydroxyl groups on surface of the support and (iii) the high surface area of the composite aerogels. To the best of our knowledge, the present Co/TEMPO-Cell aerogel composite is an efficient catalyst for the reduction of nitroaromatic compounds reported to date in comparison to other metals supported catalyst.

The possible mechanism for the reduction of nitrophenols and nitroaniline has been previously reported. [63], [64] The complete reduction process occurs mainly on the surface of metallic cobalt NPs supported on the surface of TEMPO-oxidized cellulose. In the reduction of nitrophenols and nitroaniline, BH_4^- acts as donor and the nitro group act as acceptor. In the first step, the nitrophenolate ion adsorbs on the surface of metallic cobalt catalyst and forms active hydrogen atoms. In the reduction process, the catalytic nanoparticles could act as an electronic relay system and speed up the electron transfer from BH_4^- to nitro groups and the catalytic system subsequently gives aminophenols and aminoaniline. The number of moles of 4-NA reduced per mole of metal catalyst per hour (turnover frequency, TOF) values was 154 and 171 h^{-1} for 4-NA and 2-NP, respectively. This TOF difference

between 4-NP and 2-NP is most likely due to the existence of more electronic effect on 2-NP which makes it relatively more ease for the substrate to be adopted on the metallic cobalt nanoparticles. On the other hand, the intramolecular hydrogen bond which increases the formation and adsorption of phenolate on metallic nanoparticles. The higher TOF value of 4-NA 200 h^{-1} is most likely due to the high capacity of the nitrogen atom of the amino group to adsorb onto nanoparticles of cobalt.

C. Recyclability Study

Recycling and reusability of heterogeneous catalysts is one of the desirable aspects in commercial processes. In order to examine this issue, reusability of Co/TEMPO-Cell aerogel composite was examined towards $NaBH_4$ reduction of the three nitrophenol derivatives (4-NA, 4-NP and 2-NP). After completion of the reactions, the composite catalyst was separated from the reaction mixture by simple filtration, washed with EtOH and then dried under air atmosphere for additional using at the next runs. The obtained results show that Co/TEMPO-Cell aerogel composite was reused for 11 consecutive cycles without significant loss of its catalytic activity (Figure 6-D) for the reduction of 4-NA and in supporting data S4 for the reduction of 4-NP and 2-NP.

4. Conclusion

In this study, Co/TEMPO-Cellulose aerogel composite was prepared by simple *insitu* reduction of Co^{2+} ($CoSO_4$) in water dispersion of TEMPO oxidized-Cell using sodium borohydride $NaBH_4$ as reducing agent. The *in situ* reduction process in the presence of TEMPO oxidized-cellulose very selectively oriented the reduction reaction for the metallic particles Co^0 in the presence of $NaBH_4$ as reducing agent. With this reduction process, the formation of CoB and Co2B is not observed, and Co metal nanoparticles were formed exclusively. The catalytic activity and recyclability of this composite aerogel catalyst were studied and compared with non-supported Co metal particles. The structure of Co/TEMPO-Cell aerogel composites were investigated by means of MEB microscopy, FTIR and DRX and XPS. These analyses confirm the excellent dispersion of the Co nanoparticles in the aerogel matrix which is controlled by their interactions with cellulose functional groups (COOH, CHO and OH groups) on its surface. The catalytic performances of Co/TEMPO-Cell aerogel composites and non-supported Cobalt particles were compared by measuring the turnover frequency (TOF) obtained after catalytic reduction of three nitroarenes as model reactions. Compared to non-supported Co particles, the catalytic activity of Co/TEMPO-Cell aerogel composites was significantly higher (High TOF and high reaction kinetic for the aerogel composite versus low TOF and low reaction kinetic for the unsupported Co). The recyclability of the aerogel composite was established; the aerogel composite retains good catalytic activity even after 11 cycles without significant loss of its catalytic activity. The efficient catalytic activity of the Co/TEMPO-Cell aerogel composite may be attributed to accessible, well-dispersed, and active metallic cobalt nanoparticles present on the TEMPO-oxidized cellulose support. In this way, sustainability demands, including those associated with environmental, economic and remediation issues can be addressed by the proposed concept.

Acknowledgements

532 Authors contributions:

533 NE: Investigations, Formal analysis, original draft writing.

534 LB: Conceptualization, Supervision HK, LB, NM and PZ gratefully acknowledge the French
535 Ministry of Foreign Affairs for funding NE stay in Lille through the Toubkal PHC program.
536 Chevreul Institute (FR 2638), Ministère de l'Enseignement Supérieur de la Recherche et de
537 l'Innovation, Région Hauts de France and CNRS are also acknowledged for supporting and
538 funding partially this work.

539 PZ: Funding acquisition, Supervision, review & editing.

540 NM: Supervision, Formal analysis, review & editing.

541 HK: Funding acquisition, Conceptualization, Supervision, writing, review & editing.

542

543

544

545

Reference:

[1] P. Munnik, P. E. De Jongh, and K. P. De Jong, "Recent Developments in the Synthesis of Supported Catalysts," *Chem. Rev.*, vol. 115, no. 14, pp. 6687–6718, Jul. 2015, doi: 10.1021/CR500486U.

[2] A. Mondal, A. Mondal, B. Adhikary, and D. K. Mukherjee, "Cobalt nanoparticles as reusable catalysts for reduction of 4-nitrophenol under mild conditions," *Bull. Mater. Sci.*, vol. 40, no. 2, pp. 321–328, Apr. 2017, doi: 10.1007/S12034-017-1367-3.

[3] G. C. Y. Choo, H. Miyamura, and S. Kobayashi, "Synergistic cascade catalysis by metal nanoparticles and Lewis acids in hydrogen autotransfer," *Chem. Sci.*, vol. 6, no. 3, pp. 1719–1727, Mar. 2015, doi: 10.1039/C4SC03627A.

[4] P. Mondal, A. Sinha, N. Salam, A. S. Roy, N. R. Jana, and S. M. Islam, "Enhanced catalytic performance by copper nanoparticle–graphene based composite," *RSC Adv.*, vol. 3, no. 16, pp. 5615–5623, Mar. 2013, doi: 10.1039/C3RA23280H.

[5] R. García-Álvarez, A. E. Díaz-Álvarez, P. Crochet, and V. Cadierno, "Ruthenium-catalyzed one-pot synthesis of primary amides from aldehydes in water," *RSC Adv.*, vol. 3, no. 17, pp. 5889–5894, Apr. 2013, doi: 10.1039/C3RA23195J.

[6] M. Hu, J. Sen Jiang, F. X. Bu, X. L. Cheng, C. C. Lin, and Y. Zeng, "Hierarchical magnetic iron (III) oxides prepared by solid-state thermal decomposition of coordination polymers," *RSC Adv.*, vol. 2, no. 11, pp. 4782–4786, Jun. 2012, doi: 10.1039/C2RA01190E/.

[7] Y. W. C. Cao, R. Jin, and C. A. Mirkin, "Nanoparticles with Raman spectroscopic fingerprints for DNA and RNA detection," *Science*, vol. 297, no. 5586, pp. 1536–1540, Aug. 2002, doi: 10.1126/SCIENCE.297.5586.1536.

[8] M. Kaushik and A. Moores, "Review: Nanocelluloses as versatile supports for metal nanoparticles and applications in catalysis," *Green Chem.*, vol. 18, no. 3, pp. 622–637, 2016, doi: 10.1039/C5GC02500A.

[9] W. H. Eisa, A. M. Abdelgawad, and O. J. Rojas, "Solid-State Synthesis of Metal Nanoparticles Supported on Cellulose Nanocrystals and Their Catalytic Activity," *ACS Sustain. Chem. Eng.*, vol. 6, no. 3, pp. 3974–3983, 2018, doi: 10.1021/acssuschemeng.7b04333.

[10] P. Munnik, P. E. De Jongh, and K. P. De Jong, "Recent Developments in the Synthesis of Supported Catalysts," *Chem. Rev.*, vol. 115, no. 14, pp. 6687–6718, 2015, doi: 10.1021/cr500486u.

[11] M. Gopiraman, D. Deng, S. Saravanamoorthy, I. M. Chung, and I. S. Kim, "Gold, silver and nickel nanoparticle anchored cellulose nanofiber composites as highly active catalysts for the rapid and selective reduction of nitrophenols in water," *RSC Adv.*, vol. 8, no. 6, pp. 3014–3023, Jan. 2018, doi: 10.1039/C7RA10489H.

[12] J. Gu, C. Hu, W. Zhang, and A. B. Dichiara, "Reagentless preparation of shape memory cellulose nanofibril aerogels decorated with Pd nanoparticles and their application in dye discoloration," *Appl. Catal. B Environ.*, vol. 237, pp. 482–490, Dec.

2018, doi: 10.1016/J.APCATB.2018.06.002.
[13] M. Nasrollahzadeh, N. Shafiei, Z. Nezafat, N. S. Soheili Bidgoli, and F. Soleimani, "Recent progresses in the application of cellulose, starch, alginate, gum, pectin, chitin and chitosan based (nano)catalysts in sustainable and selective oxidation reactions: A review," *Carbohydr. Polym.*, vol. 241, p. 116353, Aug. 2020, doi: 10.1016/J.CARBPOL.2020.116353.
[14] S. Jeremic *et al.*, "Production of bacterial nanocellulose (BNC) and its application as a solid support in transition metal catalysed cross-coupling reactions," *Int. J. Biol. Macromol.*, vol. 129, pp. 351–360, May 2019, doi: 10.1016/J.IJBIOMAC.2019.01.154.
[15] Q. Zhang, L. Zhang, W. Wu, and H. Xiao, "Methods and applications of nanocellulose loaded with inorganic nanomaterials: A review," *Carbohydr. Polym.*, vol. 229, p. 115454, Feb. 2020, doi: 10.1016/J.CARBPOL.2019.115454.
[16] N. Rajesh, N. Barsu, and B. Sundararaju, "Recent advances in C(sp3)H bond carbonylation by first row transition metals," *Tetrahedron Lett.*, vol. 59, no. 10, pp. 862–868, Mar. 2018, doi: 10.1016/J.TETLET.2018.01.065.
[17] A. Singh and L. Spiccia, "Water oxidation catalysts based on abundant 1st row transition metals," *Coord. Chem. Rev.*, vol. 257, no. 17–18, pp. 2607–2622, Sep. 2013, doi: 10.1016/J.CCR.2013.02.027.
[18] P. Hu and M. Long, "Cobalt-catalyzed sulfate radical-based advanced oxidation: A review on heterogeneous catalysts and applications," *Appl. Catal. B Environ.*, vol. 181, pp. 103–117, Feb. 2016, doi: 10.1016/J.APCATB.2015.07.024.
[19] S. Dey and G. C. Dhal, "The catalytic activity of cobalt nanoparticles for low-temperature oxidation of carbon monoxide," *Mater. Today Chem.*, vol. 14, p. 100198, Dec. 2019, doi: 10.1016/J.MTCHEM.2019.100198.
[20] B. Sun, T. Yoshino, S. Matsunaga, and M. Kanai, "Air-Stable Carbonyl(pentamethylcyclopentadienyl)cobalt Diiodide Complex as a Precursor for Cationic (Pentamethylcyclopentadienyl)cobalt(III) Catalysis: Application for Directed C-2 Selective C?H Amidation of Indoles," *Adv. Synth. Catal.*, vol. 356, no. 7, pp. 1491–1495, May 2014, doi: 10.1002/ADSC.201301110.
[21] S. Prakash, R. Kuppusamy, and C. H. Cheng, "Cobalt-Catalyzed Annulation Reactions via C−H Bond Activation," *ChemCatChem*, vol. 10, no. 4, pp. 683–705, Feb. 2018, doi: 10.1002/CCTC.201701559.
[22] Y. Park, Y. Kim, and S. Chang, "Transition Metal-Catalyzed C–H Amination: Scope, Mechanism, and Applications," *Chem. Rev.*, vol. 117, no. 13, pp. 9247–9301, Jul. 2017, doi: 10.1021/ACS.CHEMREV.6B00644.
[23] X. Jiang *et al.*, "Cobalt(III)-catalyzed fast and solvent-free C-H allylation of indoles using mechanochemistry," *J. Org. Chem.*, vol. 82, no. 19, pp. 10665–10672, Oct. 2017, doi: 10.1021/ACS.JOC.7B01695/SUPPL_FILE/JO7B01695_SI_001.PDF.
[24] K. Sakata, M. Eda, Y. Kitaoka, T. Yoshino, and S. Matsunaga, "Cp∗CoIII-Catalyzed C-H Alkenylation/Annulation Reactions of Indoles with Alkynes: A DFT Study," *J. Org. Chem.*, vol. 82, no. 14, pp. 7379–7387, Jul. 2017, doi: 10.1021/ACS.JOC.7B01047/SUPPL_FILE/JO7B01047_SI_001.PDF.

[25] P. G. Chirila and C. J. Whiteoak, “Recent advances using [Cp*Co(CO)I2] catalysts as a powerful tool for C–H functionalisation,” *Dalt. Trans.*, vol. 46, no. 30, pp. 9721–9739, Aug. 2017, doi: 10.1039/C7DT01980G.

[26] Y. Kommagalla and N. Chatani, “Cobalt(II)-catalyzed CH functionalization using an N,N′-bidentate directing group,” *Coord. Chem. Rev.*, vol. 350, pp. 117–135, Nov. 2017, doi: 10.1016/J.CCR.2017.06.018.

[27] J. Majewska and B. Michalkiewicz, “Low temperature one-step synthesis of cobalt nanowires encapsulated in carbon,” *Appl. Phys. A Mater. Sci. Process.*, vol. 111, no. 4, pp. 1013–1016, Jun. 2013, doi: 10.1007/S00339-013-7698-Z/FIGURES/4.

[28] M. Pudukudy and Z. Yaakob, “Methane decomposition over Ni, Co and Fe based monometallic catalysts supported on sol gel derived SiO2 microflakes,” *Chem. Eng. J.*, vol. 262, pp. 1009–1021, Feb. 2015, doi: 10.1016/J.CEJ.2014.10.077.

[29] Y. C. Liu, J. A. Koza, and J. A. Switzer, “Conversion of electrodeposited Co(OH)2 to CoOOH and Co3O4, and comparison of their catalytic activity for the oxygen evolution reaction,” *Electrochim. Acta*, vol. 140, pp. 359–365, Sep. 2014, doi: 10.1016/J.ELECTACTA.2014.04.036.

[30] J. Wang *et al.*, “Synergistic effect of two actions sites on cobalt oxides towards electrochemical water-oxidation,” *Nano Energy*, vol. 42, pp. 98–105, Dec. 2017, doi: 10.1016/J.NANOEN.2017.10.044.

[31] Y. P. Zhu, T. Y. Ma, M. Jaroniec, and S. Z. Qiao, “ Self-Templating Synthesis of Hollow Co 3 O 4 Microtube Arrays for Highly Efficient Water Electrolysis ,” *Angew. Chemie*, vol. 129, no. 5, pp. 1344–1348, Jan. 2017, doi: 10.1002/ANGE.201610413.

[32] X. Yang *et al.*, “Highly acid-durable carbon coated Co3O4 nanoarrays as efficient oxygen evolution electrocatalysts,” *Nano Energy*, vol. 25, pp. 42–50, Jul. 2016, doi: 10.1016/J.NANOEN.2016.04.035.

[33] Y. Dou *et al.*, “Graphene-like holey Co3O4 nanosheets as a highly efficient catalyst for oxygen evolution reaction,” *Nano Energy*, vol. 30, pp. 267–275, Dec. 2016, doi: 10.1016/J.NANOEN.2016.10.020.

[34] H. Zhao, J. Hao, Y. Ban, Y. Sha, H. Zhou, and Q. Liu, “Novel and efficient cobalt catalysts synthesized by one-step solution phase reduction for the conversion of biomass derived ethyl levulinate,” *Catal. Today*, vol. 319, pp. 145–154, Jan. 2019, doi: 10.1016/J.CATTOD.2018.08.011.

[35] D. Wang, J. Zhou, J. Li, X. Jiang, Y. Wang, and F. Gao, “Cobalt-boron nanoparticles anchored on graphene as anode of lithium ion batteries,” *Chem. Eng. J.*, vol. 360, pp. 271–279, Mar. 2019, doi: 10.1016/J.CEJ.2018.11.238.

[36] A. Bendahou, Y. Habibi, H. Kaddami, and A. Dufresne, “Physico-chemical characterization of palm from Phoenix Dactylifera-L, preparation of cellulose whiskers and natural rubber-based nanocomposites,” *J. Biobased Mater. Bioenergy*, vol. 3, no. 1, pp. 81–90, 2009, doi: 10.1166/JBMB.2009.1011.

[37] A. Sbiai, H. Kaddami, H. Sautereau, A. Maazouz, and E. Fleury, “TEMPO-mediated oxidation of lignocellulosic fibers from date palm leaves,” *Carbohydr. Polym.*, vol. 86, no. 4, pp. 1445–1450, Oct. 2011, doi: 10.1016/J.CARBPOL.2011.06.005.

672 [38] K. Benhamou, A. Dufresne, A. Magnin, G. Mortha, and H. Kaddami, “Control of size
673 and viscoelastic properties of nanofibrillated cellulose from palm tree by varying the
674 TEMPO-mediated oxidation time,” *Carbohydr. Polym.*, vol. 99, pp. 74–83, Jan. 2014,
675 doi: 10.1016/J.CARBPOL.2013.08.032.
676 [39] T. Saito *et al.*, “Individualization of Nano-Sized Plant Cellulose Fibrils by Direct
677 Surface Carboxylation Using TEMPO Catalyst under Neutral Conditions,”
678 *Biomacromolecules*, vol. 10, no. 7, pp. 1992–1996, Jul. 2009, doi:
679 10.1021/BM900414T.
680 [40] D. Bendahou, A. Bendahou, B. Seantier, Y. Grohens, and H. Kaddami, “Nano-
681 fibrillated cellulose-zeolites based new hybrid composites aerogels with super thermal
682 insulating properties,” *Ind. Crops Prod.*, vol. 65, pp. 374–382, Mar. 2015, doi:
683 10.1016/J.INDCROP.2014.11.012.
684 [41] M. Alle, S. C. Park, R. Bandi, S. H. Lee, and J. C. Kim, “Rapid in-situ growth of gold
685 nanoparticles on cationic cellulose nanofibrils: Recyclable nanozyme for the
686 colorimetric glucose detection,” *Carbohydr. Polym.*, vol. 253, no. July 2020, p.
687 117239, 2021, doi: 10.1016/j.carbpol.2020.117239.
688 [42] M. Alle, R. Bandi, G. Sharma, S. H. Lee, and J. C. Kim, “Shape recoverable, Au
689 nanoparticles loaded nanocellulose foams as a recyclable catalyst for the dynamic and
690 batch discoloration of dyes,” *Carbohydr. Polym.*, vol. 258, no. November 2020, p.
691 117693, 2021, doi: 10.1016/j.carbpol.2021.117693.
692 [43] K. Zhang, M. Shen, H. Liu, S. Shang, D. Wang, and H. Liimatainen, “Facile synthesis
693 of palladium and gold nanoparticles by using dialdehyde nanocellulose as template and
694 reducing agent,” *Carbohydr. Polym.*, vol. 186, pp. 132–139, Apr. 2018, doi:
695 10.1016/J.CARBPOL.2018.01.048.
696 [44] Y. He, H. Li, X. Fei, and L. Peng, “Carboxymethyl cellulose/cellulose nanocrystals
697 immobilized silver nanoparticles as an effective coating to improve barrier and
698 antibacterial properties of paper for food packaging applications,” *Carbohydr. Polym.*,
699 vol. 252, no. September, p. 117156, 2021, doi: 10.1016/j.carbpol.2020.117156.
700 [45] D. Musino, C. Rivard, G. Landrot, B. Novales, T. Rabilloud, and I. Capron, “Hydroxyl
701 groups on cellulose nanocrystal surfaces form nucleation points for silver nanoparticles
702 of varying shapes and sizes,” *J. Colloid Interface Sci.*, vol. 584, pp. 360–371, 2021,
703 doi: 10.1016/j.jcis.2020.09.082.
704 [46] J. Meng, Y. Liu, X. Shi, W. Chen, X. Zhang, and H. Yu, “Recyclable nanocellulose-
705 confined palladium nanoparticles with enhanced room-temperature catalytic activity
706 and chemoselectivity,” *Sci. China Mater.*, vol. 64, no. 3, pp. 621–630, 2021, doi:
707 10.1007/s40843-020-1438-9.
708 [47] A. Dutta *et al.*, “Copper Nanoparticles Immobilized on Nanocellulose: A Novel and
709 Efficient Heterogeneous Catalyst for Controlled and Selective Oxidation of Sulfides
710 and Alcohols,” *Catal. Letters*, vol. 149, no. 1, pp. 141–150, 2019, doi: 10.1007/s10562-
711 018-2615-x.
712 [48] M. Goswami and A. M. Das, “Synthesis of cellulose impregnated copper nanoparticles
713 as an efficient heterogeneous catalyst for C–N coupling reactions under mild

conditions," *Carbohydr. Polym.*, vol. 195, no. April, pp. 189–198, 2018, doi: 10.1016/j.carbpol.2018.04.033.
[49] M. Z. Rong, M. Q. Zhang, H. B. Wang, and H. M. Zeng, "Surface modification of magnetic metal nanoparticles through irradiation graft polymerization," *Appl. Surf. Sci.*, vol. 200, no. 1–4, pp. 76–93, Nov. 2002, doi: 10.1016/S0169-4332(02)00620-7.
[50] X. Li *et al.*, "Hybridization of inorganic CoB noncrystal with graphene and its Kubas-enhanced hydrogen," *RSC Adv.*, vol. 6, no. December 2017, pp. 93238–93244, 2016, doi: 10.1039/C6RA19238F.
[51] S. Karami, B. Zeynizadeh, and Z. Shokri, "Cellulose supported bimetallic Fe–Cu nanoparticles: a magnetically recoverable nanocatalyst for quick reduction of nitroarenes to amines in water," *Cellul. 2018 256*, vol. 25, no. 6, pp. 3295–3305, Apr. 2018, doi: 10.1007/S10570-018-1809-0.
[52] H. Heidari, "Ag Nanoparticle/Nanofibrillated Cellulose Composite as an Effective and Green Catalyst for Reduction of 4-Nitrophenol," *J. Clust. Sci. 2018 293*, vol. 29, no. 3, pp. 475–481, Feb. 2018, doi: 10.1007/S10876-018-1351-0.
[53] J. Lu, D. B. Dreisinger, and W. C. Cooper, "Cobalt precipitation by reduction with sodium borohydride," *Hydrometallurgy*, vol. 45, no. 3, pp. 305–322, Jul. 1997, doi: 10.1016/S0304-386X(96)00086-2.
[54] S. Gupta, N. Patel, A. Miotello, and D. C. Kothari, "Cobalt-Boride: An efficient and robust electrocatalyst for Hydrogen Evolution Reaction," *J. Power Sources*, vol. 279, pp. 620–625, Apr. 2015, doi: 10.1016/J.JPOWSOUR.2015.01.009.
[55] Y. D. Wang, X. P. Ai, Y. L. Cao, and H. X. Yang, "Exceptional electrochemical activities of amorphous Fe–B and Co–B alloy powders used as high capacity anode materials," *Electrochem. commun.*, vol. 6, no. 8, pp. 780–784, Aug. 2004, doi: 10.1016/J.ELECOM.2004.06.002.
[56] "CRC Handbook of Chemistry and Physics, 88th ed Editor-in-Chief: David R. Lide (National Institute of Standards and Technology) CRC Press/Taylor & Francis Group: Boca Raton, FL. 2007. 2640 pp. $139.95. ISBN 0-8493-0488-1.," *J. Am. Chem. Soc.*, vol. 130, no. 1, pp. 382–382, Jan. 2007, doi: 10.1021/JA077011D.
[57] "CRC Handbook of Chemistry and Physics, 91st Edition - كتب Google." https://books.google.fr/books?id=oROqPwAACAAJ&dq=CRC+Handbook+of+Chemistry+and+Physics,+91th&hl=ar&sa=X&redir_esc=y (accessed Nov. 21, 2021).
[58] S. S. Djokić, "Electroless Deposition of Cobalt Using Hydrazine as a Reducing Agent," *J. Electrochem. Soc.*, vol. 144, no. 7, pp. 2358–2363, Jul. 1997, doi: 10.1149/1.1837818/XML.
[59] P. Finocchiaro *et al.*, "Synthesis and characterization of novel polyamides from new aromatic phosphonate diamine monomer," *Eur. Polym. J.*, vol. 44, no. 8, pp. 2639–2651, Aug. 2008, doi: 10.1016/J.EURPOLYMJ.2008.05.022.
[60] H. Park *et al.*, "Skin irritation and sensitization potential of oxidative hair dye substances evaluated with in vitro, in chemico and in silico test methods," *Food Chem. Toxicol.*, vol. 121, pp. 360–366, Nov. 2018, doi: 10.1016/J.FCT.2018.09.017.
[61] S. Dayan, N. Kayaci, and N. Kalaycioğlu Özpozan, "Improved performance with

molecular design of Ruthenium(II) complexes bearing diamine-based bidentate ligands as sensitizer for dye-sensitized solar cells (DSSC)," *J. Mol. Struct.*, vol. 1209, p. 127920, Jun. 2020, doi: 10.1016/J.MOLSTRUC.2020.127920.

[62] S. C. Mitchell and R. H. Waring, "Aminophenols," *Ullmann's Encycl. Ind. Chem.*, Sep. 2000, doi: 10.1002/14356007.A02_099.

[63] B. Naik, S. Hazra, V. S. Prasad, and N. N. Ghosh, "Short Communication," *Catal. Commun.*, vol. 12, no. 12, pp. 1104–1108, Jul. 2011, doi: 10.1016/J.CATCOM.2011.03.028.

[64] J. Liu *et al.*, "A thermosensitive hydrogel carrier for nickel nanoparticles," *Colloids Interface Sci. Commun.*, vol. 4, pp. 1–4, Jan. 2015, doi: 10.1016/J.COLCOM.2014.12.001.

[65] J. Li, C. Y. Liu, and Y. Liu, "Au/graphene hydrogel: Synthesis, characterization and its use for catalytic reduction of 4-nitrophenol," *J. Mater. Chem.*, vol. 22, no. 17, pp. 8426–8430, 2012, doi: 10.1039/c2jm16386a.

[66] Y. C. Chang and D. H. Chen, "Catalytic reduction of 4-nitrophenol by magnetically recoverable Au nanocatalyst," *J. Hazard. Mater.*, vol. 165, no. 1–3, pp. 664–669, 2009, doi: 10.1016/j.jhazmat.2008.10.034.

[67] W. Yan *et al.*, "Facile and green synthesis of cellulose nanocrystal-supported gold nanoparticles with superior catalytic activity," *Carbohydr. Polym.*, vol. 140, pp. 66–73, 2016, doi: 10.1016/j.carbpol.2015.12.049.

[68] K. Kuroda, T. Ishida, and M. Haruta, "Reduction of 4-nitrophenol to 4-aminophenol over Au nanoparticles deposited on PMMA," *J. Mol. Catal. A Chem.*, vol. 298, no. 1–2, pp. 7–11, 2009, doi: 10.1016/j.molcata.2008.09.009.

[69] X. An, Y. Long, and Y. Ni, "Cellulose nanocrystal/hexadecyltrimethylammonium bromide/silver nanoparticle composite as a catalyst for reduction of 4-nitrophenol," *Carbohydr. Polym.*, vol. 156, pp. 253–258, 2017, doi: 10.1016/j.carbpol.2016.08.099.

[70] N. Sahiner, "Soft and flexible hydrogel templates of different sizes and various functionalities for metal nanoparticle preparation and their use in catalysis," *Prog. Polym. Sci.*, vol. 38, no. 9, pp. 1329–1356, 2013, doi: 10.1016/j.progpolymsci.2013.06.004.

[71] N. Sahiner, H. Ozay, O. Ozay, and N. Aktas, "New catalytic route: Hydrogels as templates and reactors for in situ Ni nanoparticle synthesis and usage in the reduction of 2- and 4-nitrophenols," *Appl. Catal. A Gen.*, vol. 385, no. 1–2, pp. 201–207, 2010, doi: 10.1016/j.apcata.2010.07.004.

Teresa Cristina Fonseca Silva et al. Cellulose (2012) 19:1945–1956,

Dounia Bendahou et al. Industrial Crops and Products, 65, 2015, 374-382,

Houssine Sehaqui etComposites Science and Technology, 71 (13), 2011, 1593-1599)

795

796

797

798 **List of figures and tables:**

799

800 **Figure 1:** Optical, MEB and EDX characterizations of the TEMPO-Cell and Co/ TEMPO-
801 Cell composite aerogels;

802 **Figure 2:** TEM images of Co/ TEMPO-Cell composite aerogels and Cobalt nanoparticles
803 diameter distribution;

804 **Figure 3:** XPS of A: Co/TEMPO-Cell, B: synthesized CoB;

805 **Figure 4:** FTIR spectra of CNF and Co/ TEMPO-Cell composite aerogel.

806 **Figure 5:** DRX analyses; A: XRD of the powders obtained by the reduction of CoSO4 using
807 NaBH4 and Hydrazine; B : XRD spectra of the Co/TEMPO-Cell composite and TEMPO-Cell
808 aérogels

809 **Figure 6:** A and B : UV-Vis spectra for the reduction of 4-NA with $NaBH_4$ in aqueous
810 solution recorded every 1 min using Co/TEMPO-Cell aerogel composite and unsuported Co
811 catalysts, respectively, C: plots of $\ln[C_t/C_0]$ versus reaction time for the two reduction reaction
812 and D: results of the recyclability tests of the reduction of 4-NAwith $NaBH_4$ in presence of
813 Co/TEMPO-Cellulose

814 **Table 1:** Comparison of the metal nanoparticles size with other reported systems

815 **Table 2:** Comparison of the reducing ability of Co/TEMPO-Cell aerogel composite in

816 reduction of nitro-functionalized molecule (NFM) with other reported systems

817

818